Sequential Nutrient Uptake as a Potential Mechanism for Phytoplankton to Maintain High Primary Productivity and Balanced Nutrient Stoichiometry

Kedong Yin[1,2*], Hao Liu[1,2#] and Paul J. Harrison[3]

[1]{School of Marine Sciences, Sun Yat-sen University, Guangzhou, China}
[2]{Key Laboratory of Marine Resources and Coastal Engineering in Guangdong Province，Guangzhou, China}
[3]{Department of Earth and Ocean Sciences, University of British Columbia, Vancouver BC V6T 1Z4}
*Correspondence to: Kedong Yin, School of Marine Science, Sun Yat-sen University (East Campus), Guangzhou Higher Education Mega Center, Guangzhou, 510006, China.
Tel. +86 (0)20 3933 6536; Fax +86 (0)20 3933 6607. E-mail yinkd@mail.sysu.edu.cn
#Joint first author

Running head: sequential nutrient uptake, nutritional strategy, nutrient stoichiometry

Abstract

We hypothesize that phytoplankton have the sequential nutrient uptake strategy to maintain nutrient stoichiometry and high primary productivity in the water column. According to this hypothesis, phytoplankton take up the most limiting nutrient first until depletion, continue to drawdown non-limiting nutrients and then take up the most limiting nutrient rapidly when it is available. These processes would result in the variation of ambient nutrient ratios in the water column around the Redfield ratio. We used high resolution continuous vertical profiles of nutrients, nutrient ratios and on-board ship incubation experiments to test this hypothesis in the Strait of Georgia. At the surface in summer, ambient NO_3^- was depleted with excess PO_4^{3-} and SiO_4^- remaining, and as a result, both N:P and N:Si ratios were low. The two ratios increased to about 10:1 and 0.45:1, respectively, at 20 m. Time series of vertical profiles showed that the leftover PO_4^{3-} continued to be removed, resulting in additional phosphorus storage by phytoplankton. The N:P ratios at the nutricline in vertical profiles responded differently to mixing events. Field incubation of seawater samples also demonstrated the sequential uptake of NO_3^- (the most limiting nutrient) and then PO_4^{3-} and SiO_4^- (the non-limiting nutrients). This sequential uptake strategy allows phytoplankton to acquire additional cellular phosphorus and silicon when they are available and wait for nitrogen to become available through frequent mixing of NO_3^- (or pulsed regenerated NH_4). Thus, phytoplankton are able to maintain high productivity and balance nutrient stoichiometry by taking advantage of vigorous mixing regimes with the capacity of the stoichiometric plasticity. To our knowledge, this is the first study to show the in situ dynamics of continuous vertical profiles of N:P and N:Si ratios, which can provide insight into the in situ dynamics of nutrient stoichiometry in the water column and the inference of the transient status of phytoplankton nutrient stoichiometry in the coastal ocean.

1. Introduction

The stoichiometry of the C:N:P Redfield ratio (Redfield, 1958) remains a central tenet in oceanography as it couples ecosystem processes with ocean biogeochemistry, which is driven by physical processes in oceans. Redfield ratio of C:N:P varies widely across a wide range of environmental conditions. Laboratory cultures of phytoplankton that are in the steady state usually display variable cellular N:P ratios with the nutrient N:P supply ratios (Geider and La Roche, 2002). Recently, Martiny et al. (2013) found strong latitudinal patterns of the elemental ratios, which are closely related with ambient levels of nutrients by making comparative analysis of elemental ratios of organic matter between different latitudes. Even at a fixed site, the Bermuda Atlantic Time-Series Study Station in the North Atlantic Ocean, C: N: P ratio is quite variable (Singh et al. 2015). Four mechanisms have been proposed to explain the variability in C:N:P ratios in marine plankton, as summarized by Weber and Deutsch (2010). The first mechanism emphasizes the relationship between cellular elemental stoichiometry of phytoplankton and ambient nutrient ratios, i.e., the stoichiometry of nutrients in the water column. Based on the average Redfield ratio, this mechanism has been used to infer the most limiting nutrient for phytoplankton and to debate which nutrient, nitrogen or phosphorus, should be managed to control eutrophication effects. The second mechanism suggests that the elemental stoichiometry is taxonomy specific. Diatoms were reported to drawdown nutrients with low C:P and N:P ratios (Geider and La Roche, 2002; Elser et al., 2003; Price, 2005), while marine cyanobacteria have higher C:P and N:P ratios (Karl et al., 2001; Bertilsson et al., 2003). Such different uptake ratios of N:P by phytoplankton can influence the magnitude of ocean N-fixation (Mills and Arrigo 2010) Based on the resource allocation theory, the third proposed mechanism is the “growth rate hypothesis”, which states that the elemental stoichiometry within a cell is controlled by the biochemical allocation of resources to different growth strategies (Falkowski, 2000; Elser et

al., 2003; Klausmeier et al., 2004). Fast-growing cells may have a lower N:P ratio due to a larger allocation to P-rich assembly machinery of ribosomes (Loladze and Elser, 2011), whereas competitive equilibrium favors a greater allocation to P-poor resource acquisition machinery and therefore, higher N:P ratios. The fourth mechanism is related to the interference from dead plankton or organic detritus with the measurement of elemental composition of organic matter, and such interference is difficulty to assess due to lack of the measurements of non-living organic matters in oceans and coastal waters. However, the X-ray microanalysis (XRMA) technique was recently used to produce simultaneous quotas of C, N, O, Mg, Si, P and S in single cell organisms (Segura-Noguera et al. 2016), which will not only help to understand the fourth mechanism, but also understand the variability of stoichiometry of phytoplankton in the oceans.

In culture experiments, continuous uptake of non-limiting nutrients has been demonstrated for diatoms under N and Si limitation (Conway et al., 1976; Conway and Harrison, 1977; Harrison et al., 1989). Surge uptake of the limiting nutrient occurs when it is added to the nutrient starved phytoplankton culture, while the uptake of the non-limiting nutrient is slowed or stopped until the diatom has overcome its nutrient debt. Hence, the sequence of which nutrient is taken up first is directly related to the nutrient status of the phytoplankton. It is difficult to assess the nutritional status of phytoplankton in the field, but the application of laboratory results to the interpretation of vertical nutrient profiles can provide information on their nutritional status. To date, there have been no studies of sequential uptake of nutrients in the field using a series of high resolution vertical profiles of nutrients and their application to nutritional status of the phytoplankton.

In this study, we used high resolution continuous vertical profiles of N:P and N:Si ratios to examine how N:P and N:Si ratios respond to the mixing in a highly dynamic coastal water column and the uptake of nutrients. On-board ship incubation experiments were

conducted to support the observations of changes in vertical profiles of N:P and N:Si ratios. We constructed seven conceptual profiles to illustrate how a vertical profile of N:P ratios changes with mixing and uptake of nitrogen and phosphorus and how they could indicate the nutritional status of the phytoplankton assemblage. The conceptual model also explains how N:P ratios respond to mixing, particularly at the nutriclines (nitracline for NO_3^-, phosphacline for PO_4^{3-} and silicacline for SiO_4^-), and indicates which nutrient, NO_3^- or PO_4^{3-}, is taken up first in the water column. To our knowledge, this is the first study to show the dynamics of continuous vertical profiles of N:P and N:Si ratios and to examine responses of phytoplankton to the supply of nutrients from water column mixing. We believe that our approach can add a new dimension to examining the in situ dynamics of nutrients in the water column and illustrate the ecological role of phytoplankton stoichiometry in phytoplankton competition for nutrients.

1.1. Conceptual Model of Variability in Vertical N:P ratios

The Strait of Georgia (hereafter the Strait) is an inland sea that lies between Vancouver Island and the mainland of British Columbia (LeBlond 1983). It is an ideal area for studying the interactions between mixing, nutrient vertical profiles and phytoplankton nutrient uptake because of its relatively high biomass, frequent wind mixing and shallow (15 m) photic zone. The Strait is biologically productive, reaching a daily production of up to 5 g C m^{-2} day^{-1} and annual production of up to about >300 g C m^{-2} yr^{-1} (Harrison et al., 1983, 1991), but inorganic nitrogen is often undetectable in productive seasons in the surface layer. The nutricline sitting within the euphotic zone is often associated with the pycnocline. In the Strait, the ambient N:P ratio of nutrients is ~10:1, similar to other coastal areas (Hecky and Kilham, 1988).

We illustrate the conceptual model of variability in vertical profiles of N:P ratios based on seven (C0 to C6) vertical profiles that we encountered in our field studies and suggest events that likely occurred to produce these nutrient profiles (Fig. 1).

C0: in winter or after a strong wind speed event, the water column is homogeneously mixed, and NO_3^- and PO_4^{3-} are uniformly distributed in the water column. **C1:** with the onset of stratification, NO_3^- and PO_4^{3-} are taken up within the mixed layer. Assuming that the average nutrient uptake ratio is 16N:1P, a N:P uptake ratio that is >10:1 would decrease the ambient N:P ratio to <10:1. **C2:** the uptake of $NO_3^-$and PO_4^{3-} proceeds at a N:P ratio >10:1 until NO_3^- is just depleted. At this time the N:P ratio is near 0 and some PO_4^{3-} remains in the water column. **C3:** the remaining PO_4^{3-} is completely taken up and stored as extra/surplus intracellular PO_4^{3-}. **C4:** after cross-pycnocline mixing occurs, the ambient N:P ratio in the newly mixed water should be the same as the ratio in the deep water. As a result, the vertical profile of the N:P ratio will form a right angle on the top part of the nutricline. **C5:** depending on how long the phytoplankton are nutrient limited, their response to the mixed limiting nutrient can be different. When N deficient phytoplankton take up N only, the curve of the N:P ratio parallels the NO_3^- distribution curve and PO_4^{3-} is left behind in the water column. **C6:** on the other hand, if phytoplankton take up PO_4^{3-} before NO_3^- (e.g. if phytoplankton were severely N starved, and there is a lag in NO_3^- uptake), the N:P ratio would be higher at the nutricline than below (Fig. 1).

Similarly, this conceptual model can be applied to N, SiO_4^- and N:Si ratios. The ambient (N:Si) ratio is about 0.5:1 at 20 m in the Strait, with 20 μM NO_3^- and 40 μM SiO_4^-. As the average uptake ratio of N:Si is about 0.7-1:1 (equivalent to Si:N = 1.5-1:1) (Brzezinski, 1985), the N:Si ratio decreases with depth. SiO_4^- is rarely depleted and therefore, the N:Si ratio is mainly determined by the distribution of NO_3^-. The continuous uptake of SiO_4^- without the uptake of NO_3^- can be inferred based on the comparison between the

149 gradient of N:Si and the silicacline. For example, a sharper gradient of the N:Si ratio than the
150 silicacline would indicate the continuous uptake of SiO_4^- without the uptake of NO_3^- as in C5
151 (Fig. 1)

152 **2. Materials and Methods**

153 **2.1. Station Locations**

154 The transect started from station S2, 8 km beyond the Fraser River mouth and under
155 the influence of the river plume and extended 108 km NW to S1 (well beyond the plume) in
156 the Strait of Georgia (Fig. 2). The station numbers are consistent with previous studies (Yin et
157 al., 1997a).

158 **2.2. Sampling and Data Processing**

159 The sampling was designed to investigate the distribution of nutrients (NO_3^-, PO_4^{3-}
160 and SiO_4^-) and N:P and N:Si ratios associated with mixing processes during August 6-14,
161 1991. Data at either an anchored station for 24 h, or a transect of a few stations within 10 h
162 was used. At each station, a vertical profile (0-25 m) of temperature, salinity, *in vivo*
163 fluorescence and selected nutrients (NO_3^-+NO_2^-, PO_4^{3-} and SiO_4^-) were obtained. Only
164 vertical profiles of nutrients are presented in this study. Other data (salinity, temperature and
165 fluorescence) are published elsewhere (Yin et al., 1997a). The vertical profiling system has
166 been described in detail by Jones et al. (1991) and Yin et al. (1995a). Basically, a hose
167 connected to a water pump on deck was attached to the CTD probe or S4 (InterOcean®)
168 which has the dual function of a CTD probe and a current meter. Seawater from the pump
169 was connected into the sampling tubing of an AutoAnalyzer® on board ship for *in situ*
170 nutrient measurements, while the CTD probe was lowered slowly into the water at 1 m min^{-1}.
171 Each sampling produced a high resolution continuous vertical profile of physical and
172 biological parameters and thus the relationship between these parameters in the water column

173 can be easily recognized. Data from a vertical profile (a datum point every 3 s) were
174 smoothed over 15 s intervals. This smoothing reduced the fluctuations caused by ship's
175 motion.

176 **2.3. Analysis of Nutrients**

177 All nutrients were determined using a Technicon AutoAnalyzer II. Salinity effects on
178 nutrient analyses were tested on board ship and were found to be small. Therefore, no
179 correction was made for salinity effects. NO_3^-+NO_2^- and PO_4^{3-} were determined following the
180 procedures of Wood et al. (1967) and Hager et al. (1968), respectively. The analysis of SiO_4^-
181 was based on Armstrong et al. (1967) and ammonium analysis followed Parsons et al. (1984). A water
182 sample for particulate organic carbon and nitroeng (POC and PON) was filtered onto a GF/F filter
183 and POC/PON on the filter were analyzed with a Carlo Erba model NA 1500 NCS elemental
184 analyzer, using the dry combustion method described by Sharp (1974).

185 **2.4. Field Incubation Experiments**

186 Niskin bottles (5 L) were used to take seawater samples and the samples were
187 transferred to acid cleaned carboys (10 L). Subsamples of seawater were transferred to
188 transparent polycarbonate flasks (1 L) and placed in Plexiglas tanks. The tanks were kept at
189 the same temperature as the surface water by pumping seawater (from the ship's intake at 3
190 m) through the tank. The flasks which incubated in the tanks were wrapped with 1 or 4 layers
191 of neutral density screening which corresponded to the light intensity (50-6% of the surface
192 light) from which the samples were taken (1 or 16 m). In the nutrient enrichment
193 experiments, NO_3^-, PO_4^{3-} and SiO_4^- were all added to the sample, yielding final 20-30, 2-3
194 and 20-30 μM, respectively. For experiments with additions of a single nutrient alone or
195 multiple nutrients together, a water sample taken at Stn S1 on June 4, 1990. The sample was
196 incubated with no nutrients being added during the first 28 h (pre-incubation); after pre-
197 incubation, nutrients were added in 8 treatments: no additions, NO_3^- alone (+N), PO_4^{3-} alone

198 (+P), SiO_4^- alone (+Si), NO_3^- and PO_4^{3-} together (+N+P), NO_3^- and SiO_4^- (+N+Si), PO_4^{3-} and
199 SiO_4^- (+P+Si) and all three (+N+P+Si). The final concentrations of added NO_3^-, PO_4^{3-} and
200 SiO_4^- was 7-8, 1.3-1.6 and 10-12 μM, respectively. The incubations lasted for 24 or 96 h, and
201 subsamples were taken every 3-6 h for measurements of fluorescence and nutrients. The
202 incubation experiments were conducted in different years, but in the same season.
203 Vertical profiles and seawater samples for in-situ incubation which were used in this
204 study were collected at different stations and different sampling times. Water column
205 conditions such as salinity, temperature and fluorescence have been described in the listed
206 publications as shown in Table 1.

207 **3. Results**
208
209 **3.1. Vertical Profiles of Nutrients and Nutrient Ratios**

210 At S3 near the edge of the Fraser River plume, the profiles documented changes
211 before (T1) and after wind mixing (T7). At T1, both NO_3^- and PO_4^{3-} were low in the surface
212 layer and N:P ratios were low (<2:1) and increased to ~8:1 at 20 m (Fig. 3). At T7, higher N:P
213 ratios of 16-20:1 occurred due to an increase in NO_3^- in the deep water. SiO_4^- was ~30 μM at
214 the surface due to input from the Fraser River, and increased to 37 μM at 20 m (Fig. 3). The
215 N:P ratio curve nearly formed a right angle at the top of the nutriclines at T7 when the
216 gradient of the nitracline was larger than that of the phosphacline. At T1, the N:Si ratio was
217 near 0 because NO_3^- was near the detection limit, but started to increase along the nitracline
218 at the depth of the SiO_4^- minimum. At T7, N:Si increased more rapidly with the nitracline.
219 A strong wind speed event occurred on August 7 and the water column was mixed
220 (Yin et al., 1997b). We followed the change in the nutrient profiles and nutrient ratios from
221 S3 near the Fraser River plume, to P4 and P6 and the well beyond the plume to S1. At S3,
222 N:P ratios in the water column were >7:1 when both NO_3^- and PO_4^{3-} were high after wind
223 mixing, with N:Si ratios being <0.5:1 (Fig. 4). As the post-wind bloom of phytoplankton

developed along P4-P6 due to the newly supplied nutrients (Yin et al., 1997b), N:P ratio followed the distribution of NO_3^- at P4, and decreased to 0 as NO_3^- was depleted at the surface at P6 (Fig. 4). It was clear that little PO_4^{3-} was consumed while NO_3^- was taken up. At the same time, the silicacline deepened and paralleled the nitracline. At S1, N:P and N:Si ratios formed almost a vertical line. N:P and N:Si ratios were ~8:1 and 0.5:1, respectively, in the deep water (Fig. 4).

The time series (T1, T3, T8 and T11) of Aug 8-9 captured changes over 1 or 2 days after the wind mixing event at S1 that was well beyond the river plume (Fig. 5). At T1, N:P and N:Si ratios were ~9:1 and 0.45:1, respectively, with NO_3^- and PO_4^{3-} being 15 and 1.7 μM, respectively, at the surface. At T3, N:P ratio remained constant at ~9:1, while NO_3^- and PO_4^{3-} decreased by 10 and 1.0 μM, respectively, indicating an uptake N:P ratio of 10:1. In comparison, N:Si ratio decreased from T1 to T3 when SiO_4^- was 35 μM at T1 and decreased by >10 μM at T3, producing an uptake N:Si ratio of ~1:1. At T8, N:P ratio followed the NO_3^- distribution as NO_3^- decreased to ~0 μM at the surface while PO_4^{3-} was still ~0.5 μM. This indicated that NO_3^- uptake was more rapid than PO_4^{3-} uptake and hence NO_3^- mainly determined the ambient N:P ratios. The N:Si uptake ratio of ~1:1 continued until T8. However, at T11, the N:P ratio spiked higher in the top 5-10 m of the nutricline, suggesting a more rapid uptake of PO_4^{3-} relative to NO_3^- in the upper portion of the phosphacline (Fig. 5).

Changes in the profiles after the wind event on Aug 7 were followed over 5 days (Aug 10 – 14) at P5 that was still within the influence of the river plume as evidenced by the higher surface SiO_4^- at the surface (Fig. 6). On Aug 10-11, N:P ratios were higher at the surface where the post-wind induced bloom occurred two days earlier, suggesting that uptake of PO_4^{3-} had caught up with uptake of NO_3^-. The right angle shape of the N:P ratio on Aug 12 occurred as the nutriclines became sharper due to entrainment of nutrients. By Aug 13, more NO_3^- was taken up at depth and the N:P ratio followed the deepening of the nitracline and

249 PO_4^{3-} was left behind. On Aug 14, PO_4^{3-} started to decrease. During Aug 10-14, a minimum
250 in SiO_4^- was present at an intermediate depth (5-10 m), coinciding with the top of the
251 nitracline, and the silicacline followed the nitracline below 10 m.

252 **3.2. Changes in Nutrient Ratios During Field Incubations**

253 On deck incubation experiments were used to examine changes in uptake ratios by
254 eliminating any effects due to mixing. Ambient N:P and N:Si ratios were lower at the surface
255 than at depth, indicating higher uptake of NO_3^- at the surface. The indication of a higher
256 uptake ratio of N:P and N:Si was supported by field incubation experiments. During nutrient
257 addition (NO_3^-, PO_4^{3-} and SiO_4^-) bioassays on a sample from 1 m at P3, all nutrients
258 decreased as fluorescence increased (Fig. 7). Ambient N:P and N:Si ratios decreased to
259 almost 0.0 after 96 h, indicating more rapid uptake of NO_3^- than uptake of PO_4^{3-} and SiO_4^-.
260 The temporal decline in the N:P and N:Si ratios resembled the temporal progression during a
261 bloom as illustrated in C0-C3 of the conceptual profiles (Fig. 1) and in the water column (S3,
262 P4, P6) on August 8 (Fig. 4) and during the time series at S1 (Fig. 5). During the incubation,
263 both PO_4^{3-} and SiO_4^- continued to be drawn down after NO_3^- became undetectable (Fig. 7). In
264 an earlier incubation experiment at S3 near the end of the phytoplankton bloom on June 8,
265 PO_4^{3-} was depleted at 1 m, and both NO_3^- and SiO_4^- continued to disappear with 2 μM NO_3^-
266 and 4 μM SiO_4^- being taken up. However, for the sample taken at 16 m, PO_4^{3-} (~0.5 μM) and
267 SiO_4^- (~5 μM) continued to disappear after 1.25 μM NO_3^- was depleted after 8 h (Fig. 8).

268 The water sample at S1 on June 4 was incubated for 30 h without an addition of
269 nutrients (Fig. 9-1). The initially low NO_3^-, and PO_4^{3-} remained near depletion levels during
270 the incubation, but ambient SiO_4^- decreased from 9 to <1 μM (Fig. 9-1), which was an
271 additional 8 μM SiO_4^- taken up in excess in relation to N and P. At the end of 30 h, nutrients
272 were added (Fig. 9-2). Both ambient NO_3^- and PO_4^{3-} rapidly disappeared during the first 6 h,
273 while ambient SiO_4^- decreased little (Fig. 9-2), indicating a sequential uptake of NO_3^- and

274 PO_4^{3-} since 8 μM SiO_4^- was previously taken up as shown in Fig. 9-1. The ambient N:P ratio
275 decreased faster in the samples with a single addition of NO_3^- or PO_4^{3-} alone (+N/+P) than
276 that with additions of NO_3^- and PO_4^{3-} together (+N+P) (Fig. 9-3), suggesting an interaction
277 between the uptake of NO_3^- and PO_4^{3-}. The accumulative uptake ratio of NO_3^- to PO_4^{3-}
278 increased with time, especially when only a single nutrient was present. The ratio of ambient
279 N:Si decreased with time, and the accumulative uptake ratio of N:Si exceeded 3:1 in the
280 presence of PO_4^{3-} (Fig. 9-3).

281 **4. Discussion**
282
283 The Strait is highly productive, reaching up to 2,700 mg C $m^{-2}d^{-1}$ in August (Yin et
284 al. 1997b). This is due to pulsed nutrient supplies and multiple phytoplankton blooms in
285 the shallow photic zone interacting with wind events (Yin et al. 1997b), and fluctuations in
286 river discharge (Yin et al., 1997a; Yin et al., 1995c). Our results revealed sequential nutrient
287 uptake as a potential mechanism to optimize nutrient uptake efficiency and generate high
288 primary productivity by phytoplankton by taking advantage of pulsed nutrients in this highly
289 dynamic relatively shallow photic zone.

290 **4.1. Responses of N:P and N:Si ratios to vertical mixing and uptake of nutrients**

291 A vertical profile of N:P and N:Si ratios represents a snapshot of the mixing and the
292 uptake of N, P and Si by phytoplankton in the water column. The depletion zone of the most
293 limiting nutrient in the euphotic zone ends at a depth where the uptake of nutrients just
294 balances the upward flux of nutrients through the nutracline, as indicated in C3 in the
295 conceptual profiles (Fig. 1). Different responses of nutrient uptake to pulsed nutrients by
296 mixing appeared to depend on the previous stability of the water column, the depth of the
297 euphotic zone and nutritional status of phytoplankton. Our observations spanned all seven
298 conceptual profiles (Fig. 1) and indicated the dynamic processes influencing the sequence of
299 nutrient uptake. The change in the profiles of the N:P ratio from S3 to P6 (Fig. 4) displayed

300 the spring bloom-like progression as illustrated in conceptual profiles of C0-C3 (Fig. 1) after
301 the wind mixing event. Various responses illustrated in the conceptual profiles C4, C5 and C6
302 (Fig. 1) were observed in the observations, including the right angle in the N:P ratio (T7-Fig.
303 3, P5 Aug 12, Fig. 6), parallel lines between the nitracline and the N:P ratio curve on Aug 12,
304 (Fig. 6), and a spike in the N:P ratio curve at T11 at S1 due to continued uptake of PO_4^{3-} with
305 NO_3^- being depleted during the time period from T1 to T8 (Fig. 5), which was frequently
306 observed on Aug 10 at P5 (Fig. 6). The recycling of nutrients in different preferences such as
307 faster P regeneration than N, which in turn is recycled faster than Si, also contributes to the
308 variability of nutrient ratios as shown above.
309
310 **4.2. Sequential Nutrient Uptake for Balanced Stoichiometry and Nutritional**
311 **Optimization**
312 Phytoplankton can take advantage of the dynamic mixing regimes and optimize their
313 growth rates by taking up nutrients sequentially. The disappearance of nutrients during the
314 incubation resembled the temporal progression of a bloom as illustrated in C0-C3 of the
315 conceptual profiles (Fig. 1) and in the water column (S3, P4, P6; Fig. 4), or during the time
316 series at S1 (Fig. 5).
317 Nutrient deficiency results from a decrease in the cellular content of the limiting
318 nutrient and continuous uptake of other non-limiting nutrients. Earlier studies found that N
319 limitation results in excess cellular content of P and Si (Conway and Harrison, 1977; Healey,
320 1985; Berdalet et al., 1996). Some phytoplankton develop enhanced uptake of the limiting
321 nutrient such as NH_4 and PO_4^{3-} upon its addition after a period of nutrient limitation or
322 starvation and there is an accompanying shut down of the non-limiting nutrient (Conway et
323 al., 1976; Conway and Harrison, 1977; McCarthy and Goldman, 1979). A few hours of
324 enhanced N uptake quickly overcomes the N debt since the enhanced uptake rate is many

325 times faster than the growth rate (Conway et al., 1976). For example. enhanced uptake of
326 phosphorus could double internal P within 5 min to 4 h depending on the degree of P
327 limitation and the pulsed PO_4^{3-} (Healey, 1973). After the nutrient debt has been overcome by
328 enhanced uptake, the uptake of non-limiting nutrients returns to normal after the cell quota of
329 the limiting nutrient is maximal (Collos, 1986). The sequential uptake of a limiting nutrient
330 and then the uptake of both the non-limiting and limiting nutrient is advantageous to allow
331 phytoplankton to maintain maximum growth rates over several cell generations.

332 **4.3. Significance of Sequential Uptake of Nutrients**

333 There are two essential strategies used by phytoplankton to cope with the limiting
334 nutrient (Collos, 1986). One strategy is the 'growth' response where phytoplankton uptake of
335 the limiting nutrient and cellular growth are coupled when the limiting nutrient is available.
336 The other strategy is the "storage" response where phytoplankton have the capability of
337 accumulating large internal nutrient pools, resulting in extensive uncoupling between uptake
338 and growth, and a lag in cell division of up to 24 h following a single addition of the limiting
339 nutrient. The former strategy would have the competitive advantage under frequent pulses of
340 the limiting nutrient, whereas the latter strategy presents an ecological advantage when the
341 nutrient pulsing frequency is lower than cell division rate. A phytoplankton assemblage can
342 be assumed to contain both strategists in the water column. Phytoplankton species
343 composition in subsurface waters was more or less similar at 3 stations, S1, S2 and S3
344 considering a span of 100 km across a large salinity gradient (Clifford et al. 1992).
345 Cryptomonads and *Chrysochromulina* spp and *Micromonas pusilla* were dominant at S2, S3
346 and S1 in cell density (Clifford et al. 1992). The common diatom species included
347 *Chaetoceros spp,* and *Thalassiosira spp*. (Clifford et al. 1992), which are said to use the
348 'growth' and 'storage' strategies, respectively (Collos 1986). At Stn S2, the chlorophyll
349 maximum at 7 m on August 7 contained 4 times more phytoplankton cells than at the surface

(Clifford et al. 1992), and was frequently observed at or associated with the nutricline (Cochlan et al., 1990; Yin et al., 1997 a). Phytoplankton there could use either the 'growth' or 'storage' strategy by different species. The storage strategy of non-limiting nutrients would allow phytoplankton to utilize the limiting nutrient when it is available and thus maximize phytoplankton growth by saving the energy expenditure associated with taking up non-limiting nutrients under limiting irradiance. This may explain why there were various modes or patterns of the N:P ratio at the nutricline, which indicates the different strategies of taking up nutrients sequentially based on the nutritional status of phytoplankton. The sequential uptake strategy allows some phytoplankton species to use the "storage" capacity for non-limiting nutrients and other phytoplankton species to use the "growth" response for the most limiting nutrient when it becomes available by mixing processes.

Sequential uptake of nutrients by phytoplankton can be a fundamental mechanism in maintaining high productivity in the water column where there are frequent mixing events in coastal waters. The sequential uptake strategy largely occurs at the nutraclines near or at the bottom of the photic zone. There is a consistent association between the nutriclines and the chlorophyll maximum in various aquatic environments (Cullen, 2015) and it is also common in the Strait (Harrison et al., 1991). There is a frequent upward flux of nutrients through the nutricline due to entrainment in the Strait (Yin et al., 1995a, b and c) and by internal waves in the open ocean (Pomar et al. 2012). Phytoplankton in the chlorophyll maximum are generally exposed to nutrients and when these cells are brought up to the surface during entrainment or wind mixing (Yin et al., 1995a), they can quickly photosynthesize (Yin et al., 1995c). When phytoplankton exhaust the most limiting nutrient, their internal nutrient pool decreases and they sink down to the nutriclines, possibly due to the formation of clumps and take up the abundant nutrients there. Thus, the cycle of sequential uptake of limiting and then the non-limiting nutrients may reduce nutrient deficiency in phytoplankton.

Sequential uptake of nutrients can be an important process to maintain the phytoplankton nutrient stoichiometry. Carbon fixation continues after a nutrient becomes deficient (Elrifi and Turpin, 1985; Goldman and Dennett, 1985) and the storage of organic carbon of a higher POC:N ratio is common in phytoplankton (Healey, 1973). When phytoplankton cells with excessive organic carbon due to limitation of a nutrient, sink from the upper euphotic zone to the nutricline where light becomes limiting, uptake of other nutrients occurs by utilizing stored organic carbon, leading to an increase in the cellular N and P quotas. Thus, the ratios of carbon to other nutrients approach optimum stoichiometry. POC:N ratios at Stn S2 and S3 were observed to be between 6:1 and 7:1 in the water column, even though both ambient NO_3^- and PO_4^{3-} were near detection limits (Fig. 10). In addition, POC:N ratio was slightly higher than 7:1 (Fig. 10) at Stn S1 where nitrogen was more frequently under detection limit than Stns S2 and S3. This might suggest the lack of ambient nitrogen limitation on the cellular nutrient stoichiometry. However, using C:N ratio in particular matter to infer the nutrient limitation has its limitation as particular C:N ratios do not necessarily reflect phytoplankton elemental composition alone, especially in estuarine influenced waters.

5. Conclusion

The use of in-situ continuous vertical profiles in this study shows a high variability of ambient N:P and N:Si ratios in the water column, suggesting the dynamics of nutrient uptake ratios, as illustrated in the conceptual model of Fig. 1. The incubation experiments demonstrated the sequential uptake of nutrients by phytoplankton, which suggests that deficiency of a nutrient that is based on the ambient nutrient ratio could be transient and overcome by the sequential uptake of the most limiting nutrient and non-limiting nutrients. The capacity of sequential uptake of nutrients is an important strategy for phytoplankton to maintain high primary productivity and near optimum cellular nutrient stoichiometry in the water column. The sequential nutrient uptake strategy also offers another mechanism for the

explanation of the variability in the nutrient stoichiometry of phytoplankton in the euphotic zone.

Authors contributions

K. Yin collected data and wrote the manuscript.

PJ Harrison supported the research cruise for collection of data and designed the sampling plan.

Competing interests

The authors declare that they have no conflict of interest.

Acknowledgements

This research was funded by a Natural Sciences and Engineering Research Council of Canada (NSERC) Strategic grant awarded to Prof. Paul J. Harrison. K. Yin acknowledges the continuing support of NSFC 91328203 to this study. We thank Dr. Mike St. John who coordinated the cruise. We acknowledge the Department of Fisheries and Oceans for providing ship time, and the officers and crew of C.S.S. Vector for their assistance.

References

Armstrong, F. A. J., Stearns, C. R., and Strickland, J. D. H.: The measurement of upwelling and subsequent biological processes by means of the Technicon Autoanalyzer® and associated equipment, Deep Sea Research and Oceanographic Abstracts, 14, 381-389, 1967.

Berdalet, E., Marrasé, C., Estrada, M., Arin, L., and MacLean, M. L.: Microbial community responses to nitrogen- and phosphorus-deficient nutrient inputs: microplankton dynamics and biochemical characterization, J. Plank. Res., 18, 1627-1641, 1996.

Bertilsson, S., Berglund, O., Karl, D. M., and Chisholm, S. W.: Elemental composition of marine Prochlorococcus and Synechococcus: Implications for the ecological stoichiometry of the sea, Limnol. Oceanogr., 48, 1721-1731, 2003.

Brzezinski, M. A.: The Si:C:N ratio of marine diatoms: interspecific variability and the effect of some environmental variables, J. Phycol., 21, 247-257, 1985.

Clifford, P.J., Harrison, P.J., St. John, M.A., Yin, K., and Albright, L.J.: Plankton production and nutrient dynamics in the Fraser River plume, 1989. Manuscript Report No. 54. Department of Oceanography, University of British Columbia, Vancouver, B.C. Canada, 225 pp, 1991a.

Clifford, P.J., Harrison, P.J., Yin, K., St. John, M.A., and Goldblatt, R.H.: Plankton production and nutrient dynamics in the Fraser River plume, 1990. Manuscript Report No. 58. Department of Oceanography, University of British Columbia, Vancouver, B.C. Canada, 265 pp, 1991b.

Cochlan, W. P., Harrison, P. J., Clifford, P. J., and Yin, K.: Observations on double chlorophyll maxima in the vicinity of the Fraser River plume, Strait of Georgia, British Columbia, J. Exp. Mar. Biol. Ecol., 143, 139-146, 1990.

Collos, Y.: Time-lag algal growth dynamics: biological constraints on primary production in aquatic environments, Mar. Ecol. Prog. Ser., 33, 193-206, 1986.

Conley, D. J., Paerl, H. W., Howarth, R. W., Boesch, D. F., Seitzinger, S. P., Havens, K. E., Lancelot, C., and Likens, G. E.: Controlling eutrophication: nitrogen and phosphorus, Science, 323, 1014-1015, 2009.

Conway, H. L. and Harrison, P. J.: Marine diatoms grown in chemostats under silicate or ammonium limitation IV. Transient response of Chaetoceros debilis, Skeletonema costatum and Thalassiosira gravida to a single addition of the limiting nutrient, Mar. Biol., 43, 33-43, 1977.

Conway, H. L., Harrison, P. J., and Davis, C. O.: Marine diatoms grown in chemostats under silicate or ammonium limitation. II. Transient response of Skeletonema costatum to a single addition of the limiting nutrient, Mar. Biol., 35, 187-199, 1976.

Cullen, J.J.: Subsurface chlorophyll maximum layers: enduring enigma or mystery solved?, Annu. Rev. Mar. Sci., **7,** 207-239, 2015.

Elrifi, I. R. and Turpin, D. H.: Steady-state luxury consumption and the concept of optiumum

455 nutrient ratios: a study with phosphate and nitrate limited Selenastrum minutum
456 (Chlorophyte), J. Phycol., 21, 592-602, 1985.

457 Elser, J. K., Acharya, M., Kyle, J., Cotner, W., Makino, T., Markow, T., Watts, S., Hobbie, W.,
458 Fagan, J., Schade, J., Hood, J., and Sterner, R. W.: Growth rate-stoichiometry
459 couplings in divers biota, Ecol. Lett., 6, 936-943, 2003.

460 Falkowski, P. G.: Rationalizing elemental ratios in unicellular algae, J. Phycol., 36, 3-6, 2000.

461 Geider, R.J. and La Roche, J.: Redfield revisited: variability of C:N:P in marine microalgae
462 and its biochemical basis, Eur. J. Phycol., 37, 1-17, 2002.

463 Goldman, J. C. and Dennett, M. R.: Photosynthetic responses of 15 phytoplankton species to
464 ammonium pulsing, Mar. Ecol. Prog. Ser., 20, 259-264, 1985.

465 Hager, S. W., Gordon, L. I., and Park, P. K.: A practical manual for the use of the Technicon
466 AutoAnalyzer in seawater nutrient analysis, Final Rep. Bur. Commcr. Fish., Contract,
467 pp14-17, 1968.

468 Harrison, P.J., Parsons, T.R., Taylor, F.J.R., and Fulton, J.D.: Review of Biological
469 oceanography of the Strait of Georgia: Pelagic Environment. Can. J. Fish. Aquat.
470 Sci. 40: 1064-1094, 1983.
471
472 Harrison, P. J., Parslow, J. S., and Conway, H. L.: Determination of nutrient uptake kinetics
473 parameters: a comparison of methods, Ma.r Ecol. Prog. Ser., 52, 301-312, 1989.

474 Harrison, P. J., Clifford, P. J., Cochlan, W. P., Yin, K., St. John, M. A., Thompson, P. A.,
475 Sibbald, M. J., and Albright, L. J.: Nutrient and plankton dynamics in the Fraser-river
476 plume, Strait of Georgia, British-Columbia, Mar. Ecol. Prog. Ser., 70, 291-304, 1991.

477 Healey, F. P.: Inorganic nutrient uptake and deficiency in algae, CRC Crit. Rev. Microbiol., 3,
478 69-113, 1973.

479 Healey, F. P.: Interacting effects of light and nutrient limitation on growth rate of
480 Synechococcus linearis (Cyanophyceae), J. Phycol., 21, 134-146, 1985.

481 Hecky, R. E. and Kilham. P.: Nutrient limitation of phytoplankton in freshwater and marine
482 environments: a review of recent evidence on the effects of enrichment, Limnol.
483 Oceanogr., 33, 786-822, 1988.

484 Jones, D. M., P. J., Harrison, P. J., Clifford, P. J., Yin, K., and John, M. St.: A computer-based
485 system for the acquisition and display of continuous vertical profiles of temperature,
486 salinity, fluorescence and nutrients, Water Res., 25, 1545-1548, 1991.

487 Karl, D. M., Björkman, K. M., Dore, J. E., Fujieki, L., Hebel, D. V., Houlihan, T., Letelier, R.
488 M., and Tupas, L. M.: Ecological nitrogen-to-phosphorus stoichiometry at station
489 aloha, Deep Sea Res. PT II, 48, 1529-1566, 2001.

490 Klausmeier, C. A., Litchman, E., Daufresne, T. and Levin, S. A.: Optimal nitrogen-to-
491 phosphorus stoichiometry of phytoplankton, Nature, 429, 171-174, 2004.

492 LeBlond, P.H.: The Strait of Georgia: functional anatomy of a coastal sea. Can. J. Fish.
493 Aquat. Sci. 40, 1033-1063, 1983.

494 Loladze, I. and Elser, J.: The origins of the Redfield nitrogen-to-phosphorus ratio are in a
495 homoeostatic protein-to-rRNA ratio, Ecol. Lett., 14, 244-250, 2011.

496 Martiny, A.C., Pham, C.T. A., Primeau, F. W., Vrugt, J.A., Keith Moore. J., Levin, S.A. and
497 Lomas, M.W.: Strong latitudinal patterns in the elemental ratios of marine plankton
498 and organic matter. Nature Geoscience 6, 279-283, 2013.

499 McCarthy, J. J., and Goldman, J. C.: Nitrogenous nutrition of marine phytoplankton in
500 nutrient depleted waters, Science, 203, 670-672, 1979.

501 Mills, Matthew M, and Kevin R Arrigo (2010) Magnitude of Oceanic Nitrogen Fixation
502 Influenced by the Nutrient Uptake Ratio of Phytoplankton. Nature Geoscience 3(6):
503 412–416.

504 Pomar, L., Morsilli, M., Hallock, P. and Bádenas, B.: Internal waves, an under-explored
505 source of turbulence events in the sedimentary record. Earth-Science Reviews 111,
506 56-81, 2012.

507 Price, N. M.: The elemental stoichiometry and composition of an iron-limited diatom,
508 Limnol. Oceanogr., 50, 1159-1171, 2005.

509 Redfield, A. C.: The biological control of chemical factors in the environment, Am. Sci., 46,
510 205-222, 1958.

511 Segura-Noguera M., Blasco D., Fortuño J.-M.: Taxonomic and Environmental Variability in
512 the Elemental Composition and Stoichiometry of Individual Dinoflagellate and
513 Diatom Cells from the NW Mediterranean Sea, PLoS ONE 11(4): e0154050,
514 doi:10.1371/journal.pone.0154050, 2016.

515 Sharp, J.H.: Improved analysis of particulate organic carbon and nitrogen from seawater.
516 Limnol. Oceanogr., 19, 984-989, 1974.

517 Singh, Arvind, SE Baer, Ulf Riebesell, AC Martiny, and MW Lomas (2015) C: N: P
518 Stoichiometry at the Bermuda Atlantic Time-Series Study Station in the North
519 Atlantic Ocean. Biogeosciences 12(21): 6389–6403.

520 Wood, E. D., Armstrong, F. A. J., and Richards, F. A.: Determination of nitrate in sea water
521 by cadmium-copper reduction to nitrite, J. Mar. Biol. Ass. U.K., 47, 23-31, 1967.

522 Weber, T. S., and Deutsch, C.: Ocean nutrient ratios governed by plankton biogeography,
523 Nature, 467, 550-554, 2010.

524 Yin, K., Harrison, P. J., Pond, S., and Beamish, R. J.: Entrainment of nitrate in the Fraser
525 River plume and its biological implications. I. Effects of salt wedge, Estuar. Coast.
526 Shelf Sci., 40, 505-528, 1995a.

527 Yin, K., Harrison, P. J., Pond, S., and Beamish, R. J.: Entrainment of nitrate in the Fraser
528 River plume and its biological implications. II. Effects of spring vs neap tides and
529 river discharge, Estuar. Coast. Shelf Sci., 40, 529-544, 1995b.

530 Yin, K., Harrison, P. J., Pond, S., and Beamish, R. J.: Entrainment of nitrate in the Fraser
531 River plume and its biological implications. III. Effects of winds, Estuar. Coast. Shelf
532 Sci., 40, 545-558, 1995c.

533 Yin, K., Harrison, P. J., and Beamish, R. J.: Effects of a fluctuation in Fraser River discharge
534 of primary production in the central Strait of Georgia, British Columbia, Canada, Can.
535 J. Fish Aquat. Sci., 54, 1015-1024, 1997a.

536 Yin, K., Goldblatt, R. H., Harrison, P. J., John, M. A. St., Clifford, P. J., and Beamish, R. J.:
537 Importance of wind and river discharge in influencing nutrient dynamics and
538 phytoplankton production in summer in the central Strait of Georgia, Mar. Ecol. Prog.
539 Ser., 161, 173-183, 1997b.

540

Table 1. Water column conditions such as vertical profiles of salinity, temperature and fluorescence can be found in the listed publications for the sampled stations in the Strait of Georgia.

Stations	Sampling date	Water column conditions being described
S1 (Fig. 9）	June 4, 1990	Clifford et al. (1991b)
S3 (Fig. 3)	August 6-7, 1991	Yin et al. (1997b)
S3-P4-P6-S1 (Fig. 4)	August 8, 1991	Yin et al. (1997b).
S1 (Fig. 5)	August 8-9, 1991	Yin et al. (1997b)
P5 (Fig. 6)	August 10-14, 1991	Yin et al. (1997b)
P3 (Fig. 7)	August 11-16,1991	Yin et al. (1997b)
S3 (Fig. 8)	June 8, 1989	Clifford et al. (1991a)
S1, S2 and S3 (Fig. 10)	August 20-23, 1990	Clifford et al. (1991b)

Figures captions

Figure 1. Conceptual model for sequential nutrient uptake, which is illustrated in vertical profiles of N, P and N:P ratios. C0 to C3 represent a time series of nutrient uptake during bloom development and C4 to C6 indicate subsequent vertical mixing of nutrients and subsequent uptake. The short horizontal line near the middle of the depth axis indicates the euphotic zone depth. N disappears first at C2, and P is left which continues to be taken up at C3. C4 represents mixing of nutrients into the bottom of the photic zone and phytoplankton have not taken up these nutrients yet. At C5, N is taken up first before P, while at C6, P is taken up first before N.

Figure 2. Map of the Strait of Georgia showing the study area and the sampling stations. Note: the Fraser River is located to the right, having two river channels flowing into the Strait of Georgia.

Figure 3. Two vertical profiles (T1=12:15 and T7=06:15) in the time series for August 6-7, 1991 of nutrients at S3. Left panel: NO_3^-, PO_4^{3-} and N:P ratios. Right panel: SiO_4^- and N:Si.

Figure 4. Vertical profiles at S3 near the Fraser River plume to P4 and P6 finally to S1 that was well beyond the plume (108 km away) during August 8, 1991. Left panel: NO_3^-, PO_4^{3-} and N:P ratios. Right panel: SiO_4^- and N:Si ratios.

Figure 5. Selected vertical profiles at S1 during the time series (T1, T3, T8 and T11) of August 8-9, 1991. Left panel: NO_3, PO_4 and N:P ratios. Right panel: SiO_4^- and N:Si ratios.

Figure 6. Vertical profiles in the time series at P5 during August 10-14, 1991. Left panel: NO_3^-, PO_4^{3-} and N:P ratios. Right panel: SiO_4^- and N:Si ratios.

Figure 7. Time course of duplicate in vivo fluorescence, NO_3^-, PO_4^{3-} and SiO_4^-, and N:P and N:Si ratios during an in situ incubation of a water sample taken from 1 m at P3 on August 11 (11:45). NO_3^-, PO_4^{3-} and SiO_4^- were added to the water sample at T=0 before the incubation.

Figure 8. Time course NO_3^-, PO_4^{3-} and SiO_4^- during the field incubation of water samples taken at Stn S3 during June 8, 1989. Top panel: sample taken at 1 m and the incubation was done under 1 layer of screening. Bottom panel: sample taken at 16 m and incubated under 4 layers of screening.

Figure 9. Time course of ambient NO_3^-, PO_4^{3-}, and SiO_4^- during the field incubation of a water sample taken at Stn S1 on June 4, 1990. Fig. 9-1) pre-incubation: no nutrients were added to the sample during the first 28 h; Fig. 9-2) after pre-incubation, nutrients were added in 8 treatments: +N, +P, +Si, +N+P, +N+Si, +P+Si and +N+P+Si; Fig. 9-3) ambient nutrient ratios were calculated from measured ambient nutrients during the time course of incubation in Fig. 9-2. The sign "+" means "added". +N/+P and +N/+Si indicate the ratio of the added N alone over the added P alone and over the added Si alone, respectively. The accumulative uptake ratio was directly calculated from the decreasing concentrations over time in Fig. 9-2.

Figure 10. Vertical profiles of particulate organic C:N ratios at stations Stn S2, S3 and S1 along the increasing distance from the river during August 20-23, 1990.

Fig. 1

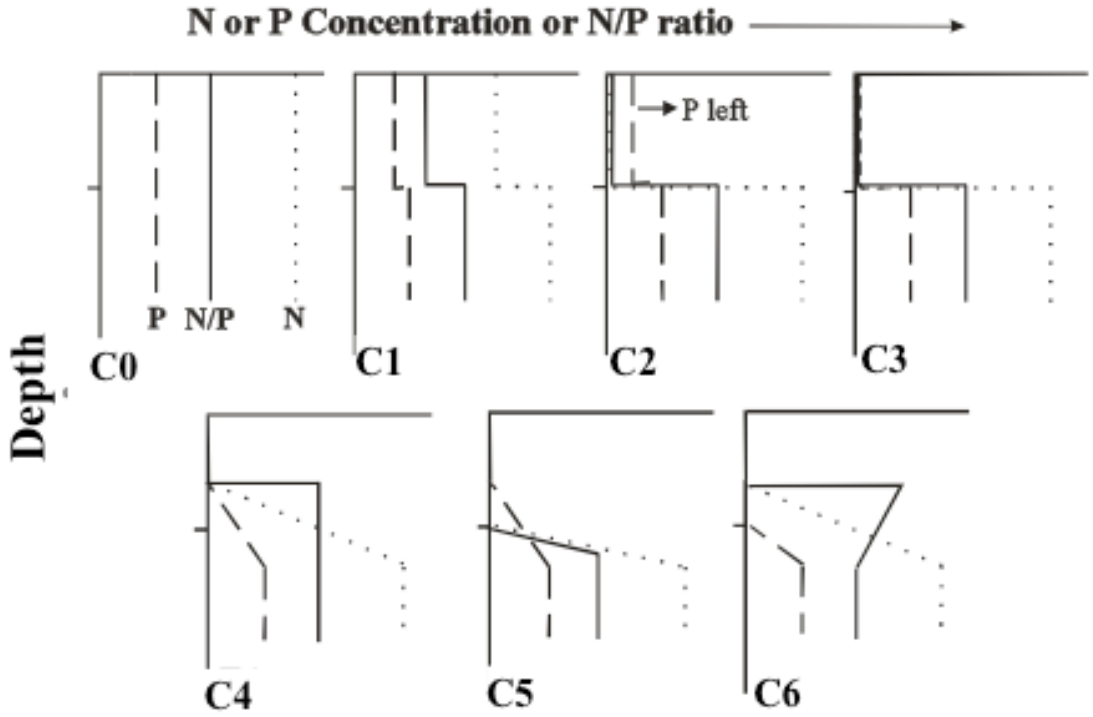
N or P Concentration or N/P ratio
Depth
P left
P
N/P
N
C0
C1
C2
C3
C4
C5
C6

Fig. 2

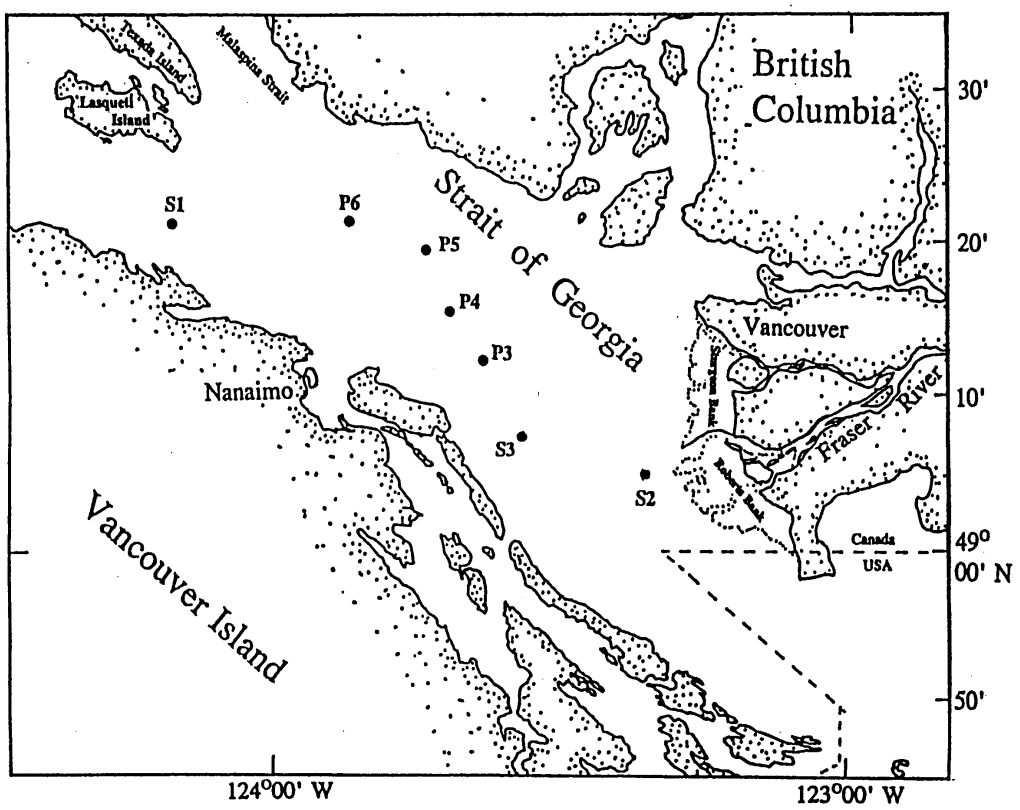
Texada Island
Malaspina Strait
Lasqueti Island
British Columbia
30'
S1
P6
P5
Strait of Georgia
20'
P4
Vancouver
P3
Nanaimo
Sturgeon Bank
Fraser River
10'
S3
S2
Roberts Bank
Canada
USA
49°
00' N
Vancouver Island
50'
124°00' W
123°00' W

Fig. 3

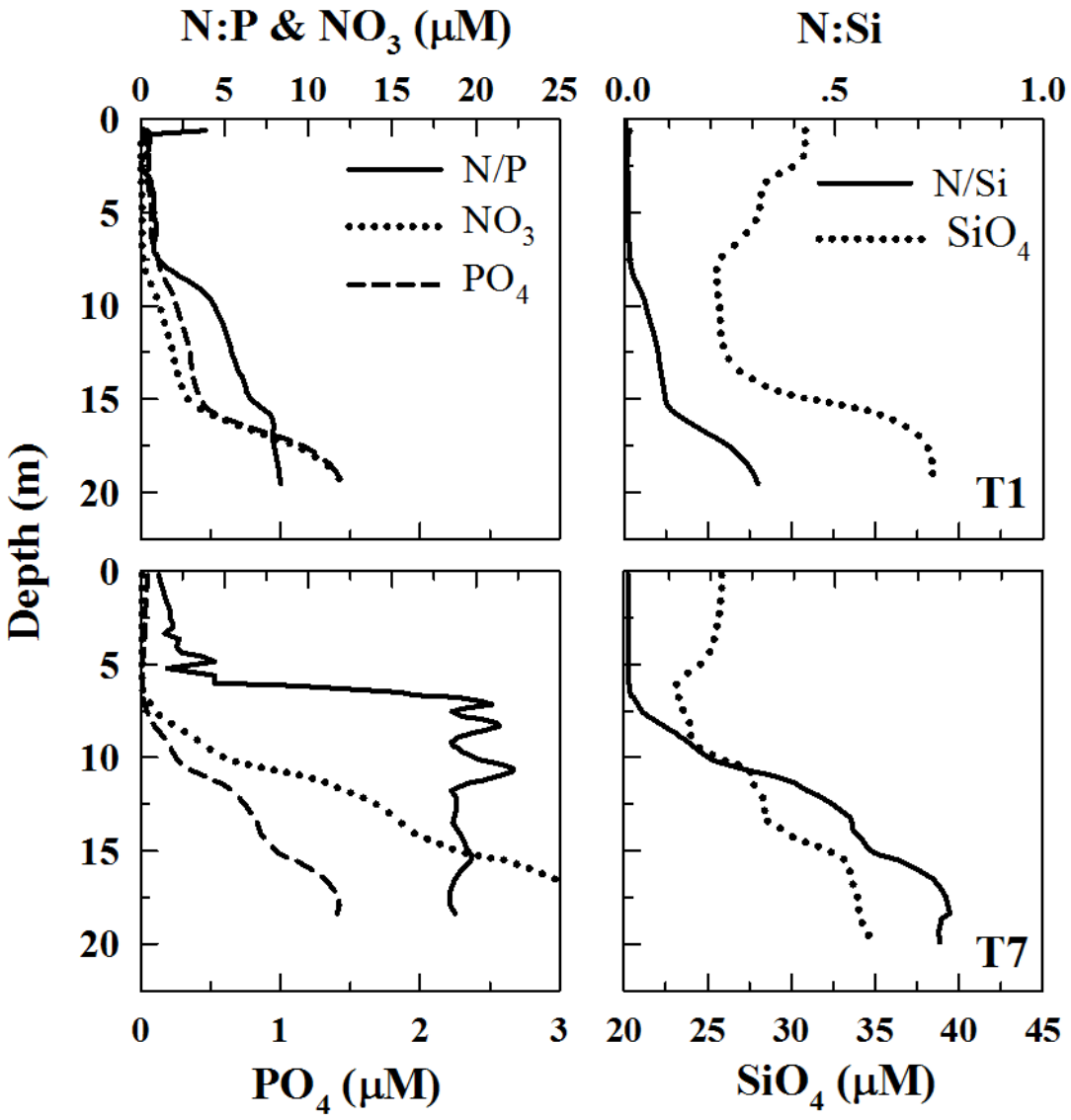

Fig. 4

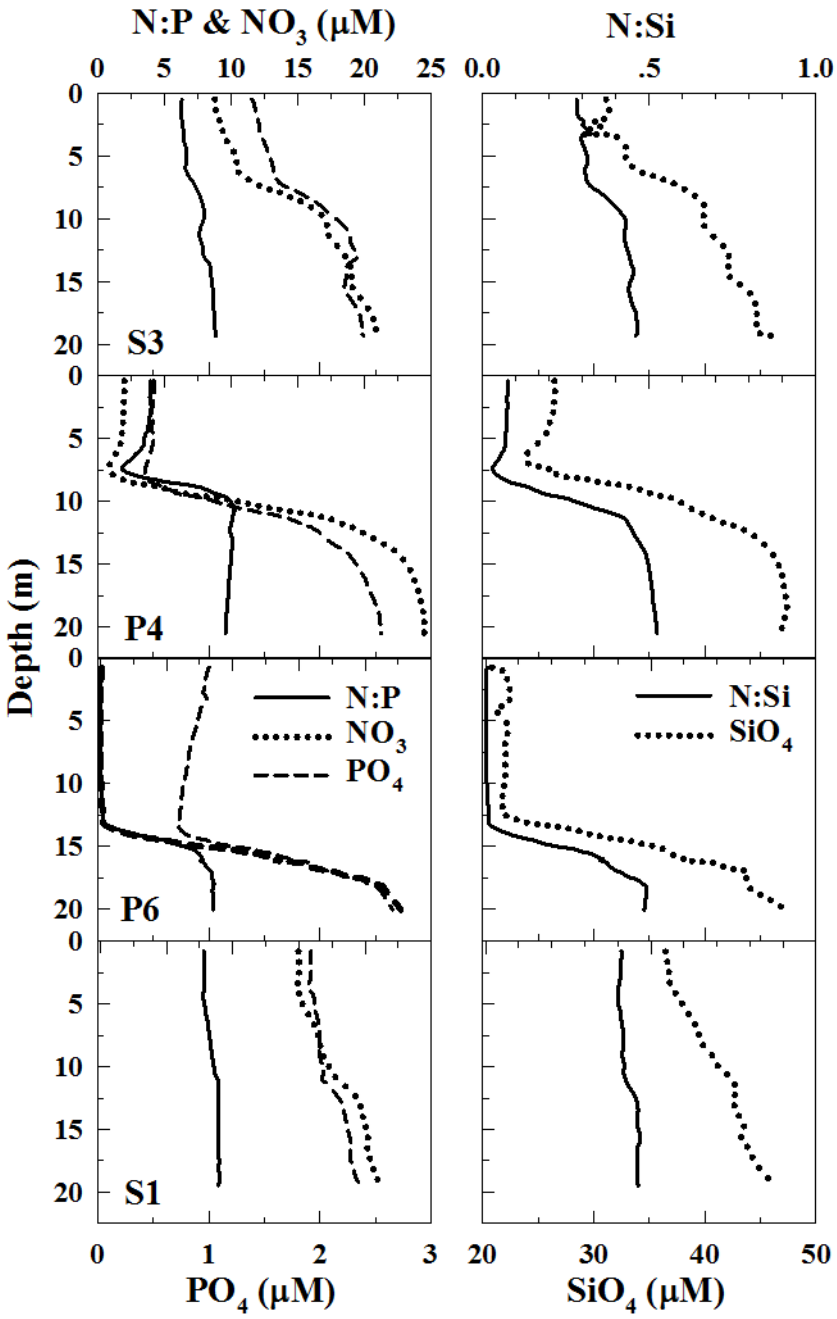
N:P & NO3 (µM)
N:Si
Depth (m)
S3
P4
P6
S1
N:P
NO3
PO4
N:Si
SiO4
PO4 (µM)
SiO4 (µM)

Fig. 5

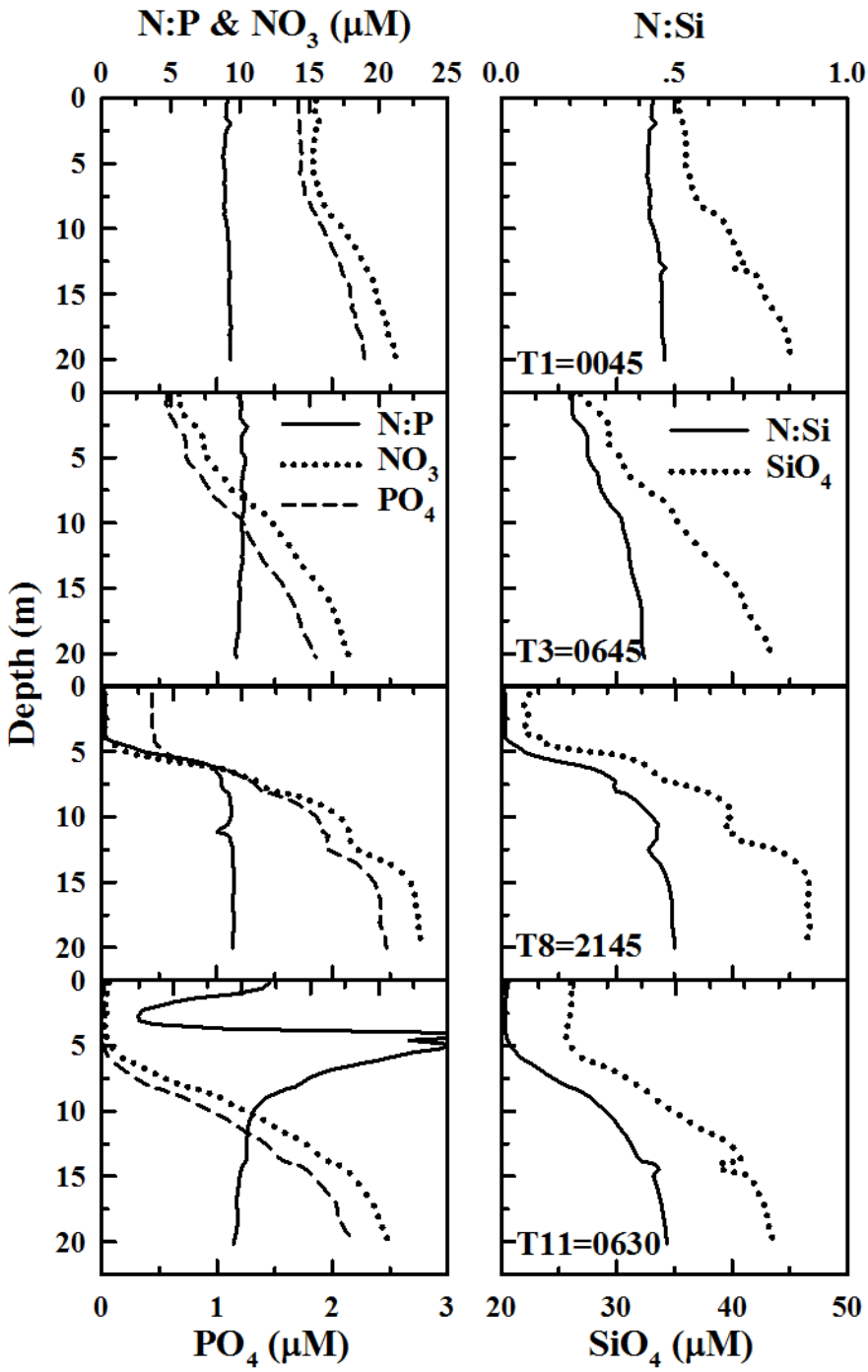
N:P & NO3 (µM)
N:Si
Depth (m)
T1=0045
T3=0645
T8=2145
T11=0630
N:P
NO3
PO4
N:Si
SiO4
PO4 (µM)
SiO4 (µM)

Fig. 6

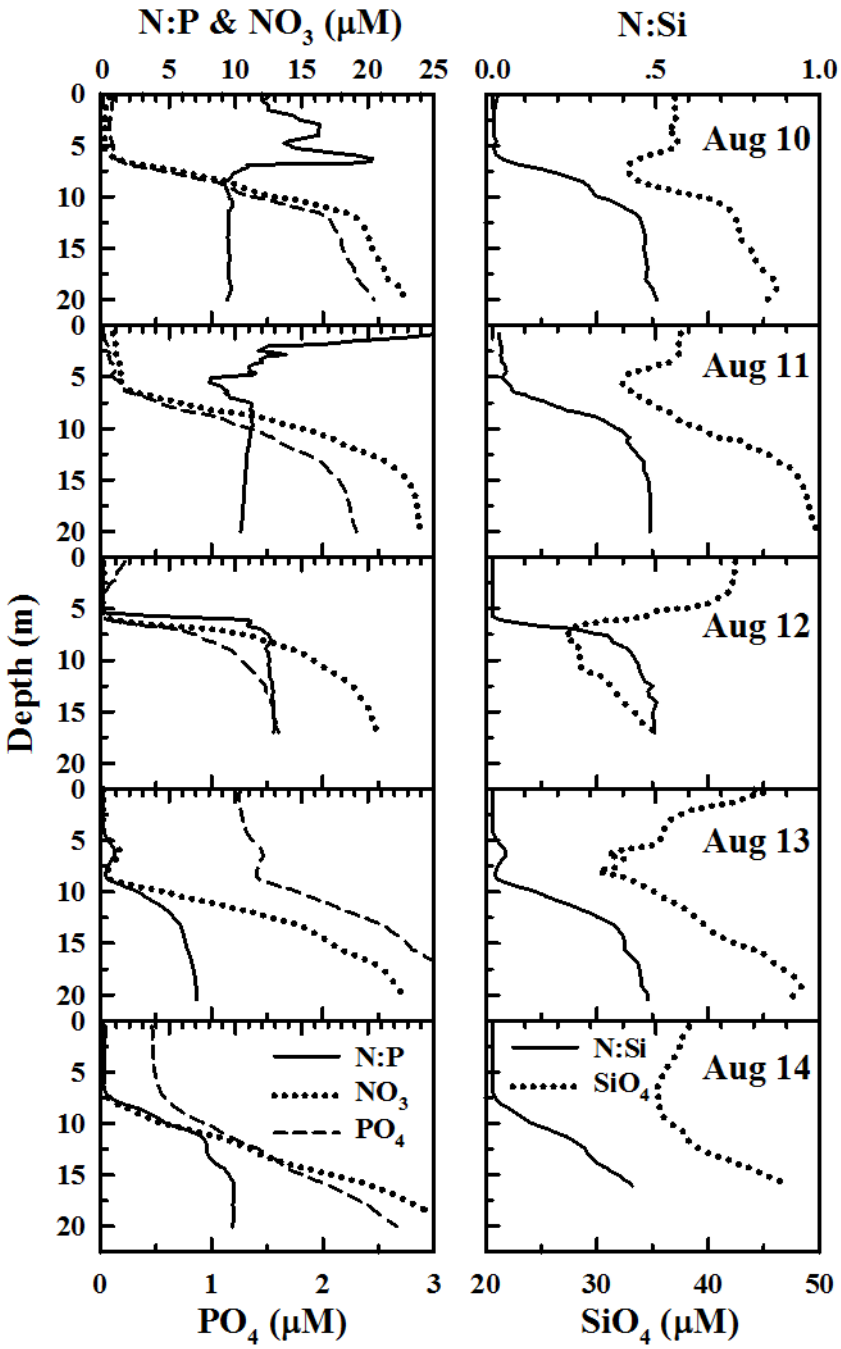
N:P & NO3 (µM)
N:Si
Depth (m)
Aug 10
Aug 11
Aug 12
Aug 13
Aug 14
N:P
NO3
PO4
N:Si
SiO4
PO4 (µM)
SiO4 (µM)

Fig. 7

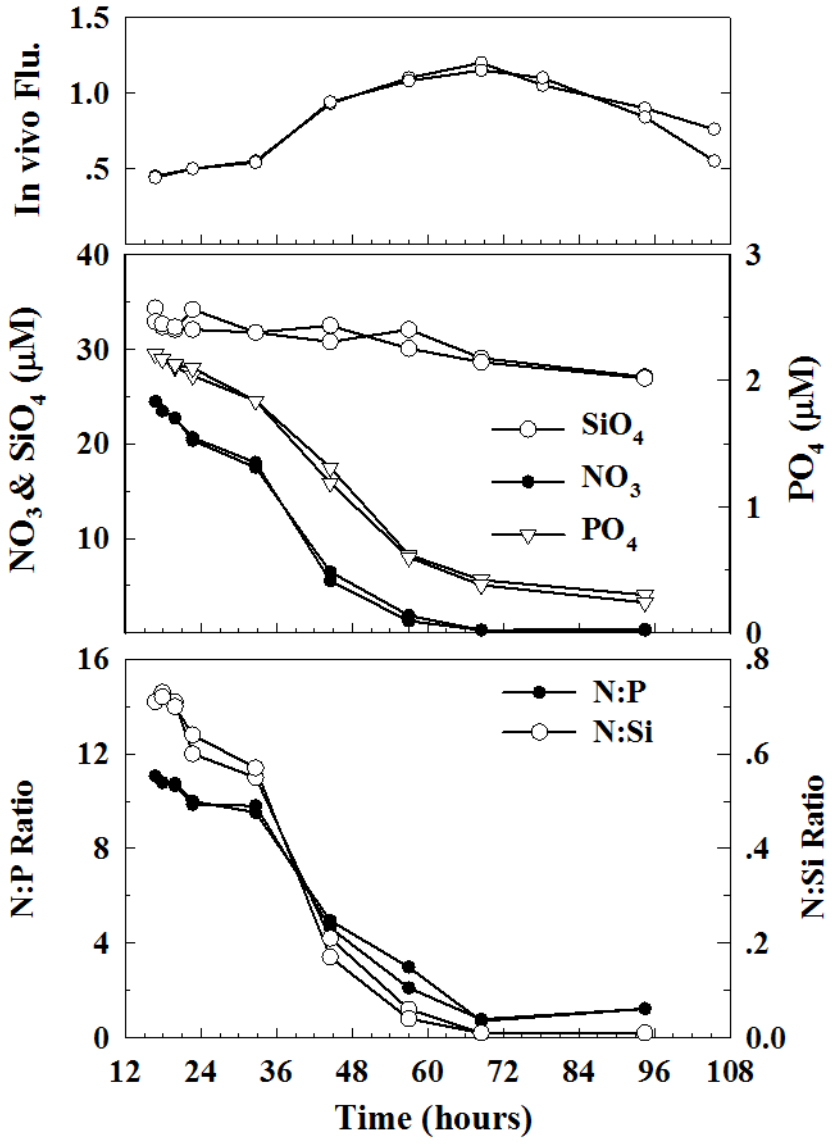
In vivo Flu.
1.5
1.0
.5
0
NO3 & SiO4 (µM)
40
30
20
10
0
PO4 (µM)
3
2
1
0
SiO4
NO3
PO4
N:P Ratio
16
12
8
4
0
N:Si Ratio
.8
.6
.4
.2
0.0
N:P
N:Si
12
24
36
48
60
72
84
96
108
Time (hours)

Fig. 8

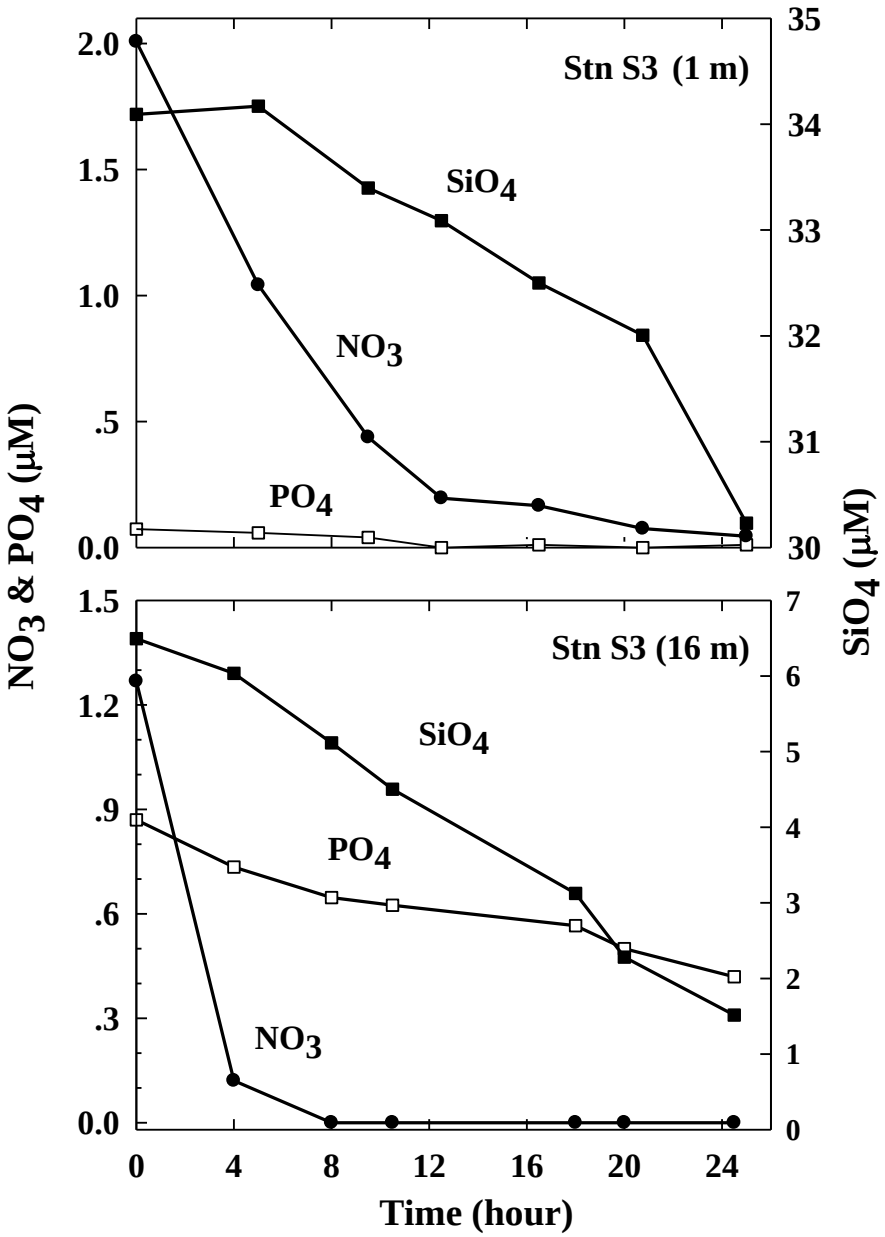
Stn S3 (1 m)
SiO4
NO3
PO4
Stn S3 (16 m)
SiO4
PO4
NO3
NO3 & PO4 (µM)
SiO4 (µM)
Time (hour)
0
4
8
12
16
20
24
2.0
1.5
1.0
.5
0.0
1.2
.9
.6
.3
35
34
33
32
31
30
7
6
5
4
3
2
1
0

Fig. 9-1

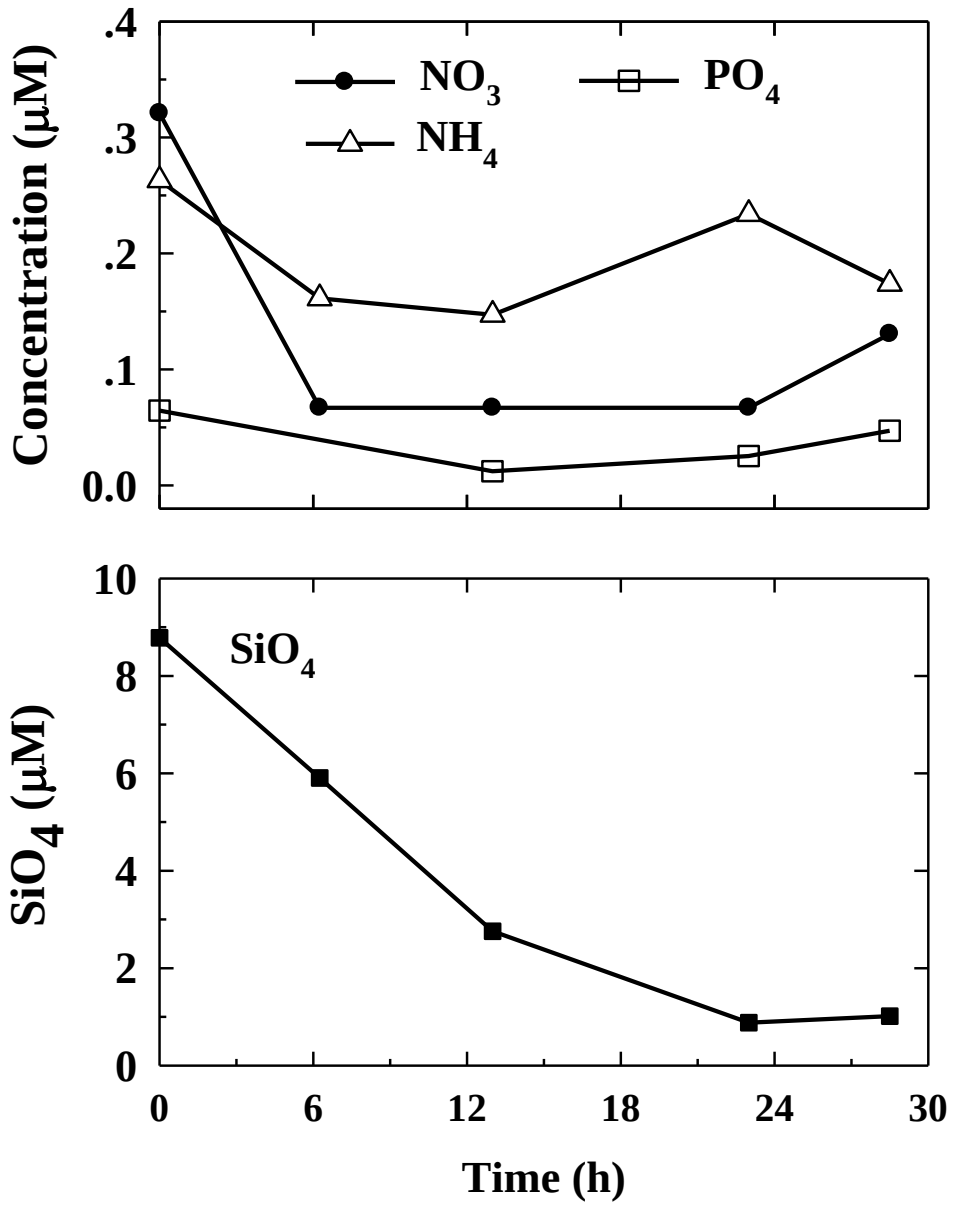
.4
.3
.2
.1
0.0
Concentration (μM)
NO3
PO4
NH4
10
8
6
4
2
0
SiO4 (μM)
SiO4
0
6
12
18
24
30
Time (h)

Fig. 9-2

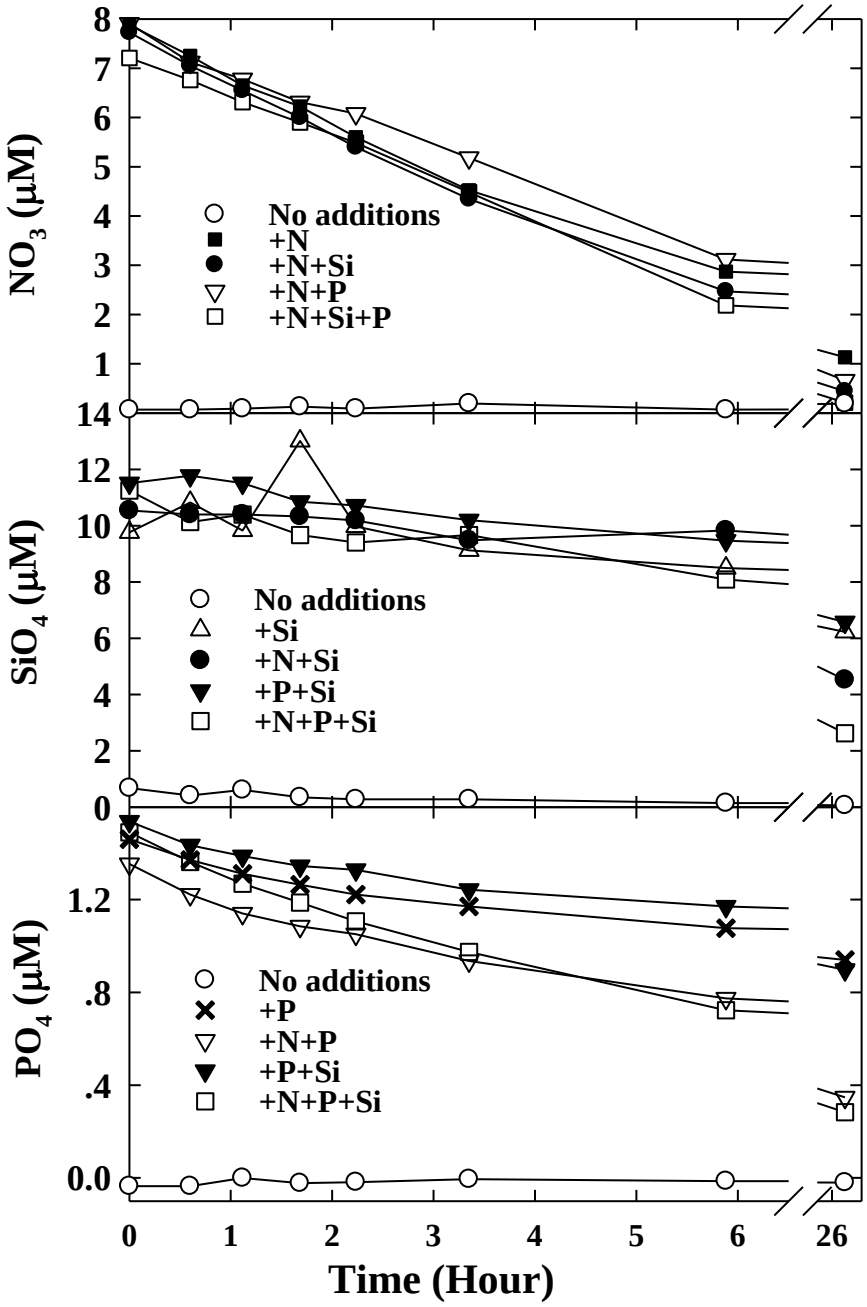
NO3 (µM)
No additions
+N
+N+Si
+N+P
+N+Si+P
SiO4 (µM)
No additions
+Si
+N+Si
+P+Si
+N+P+Si
PO4 (µM)
No additions
+P
+N+P
+P+Si
+N+P+Si
Time (Hour)

Fig. 9-3

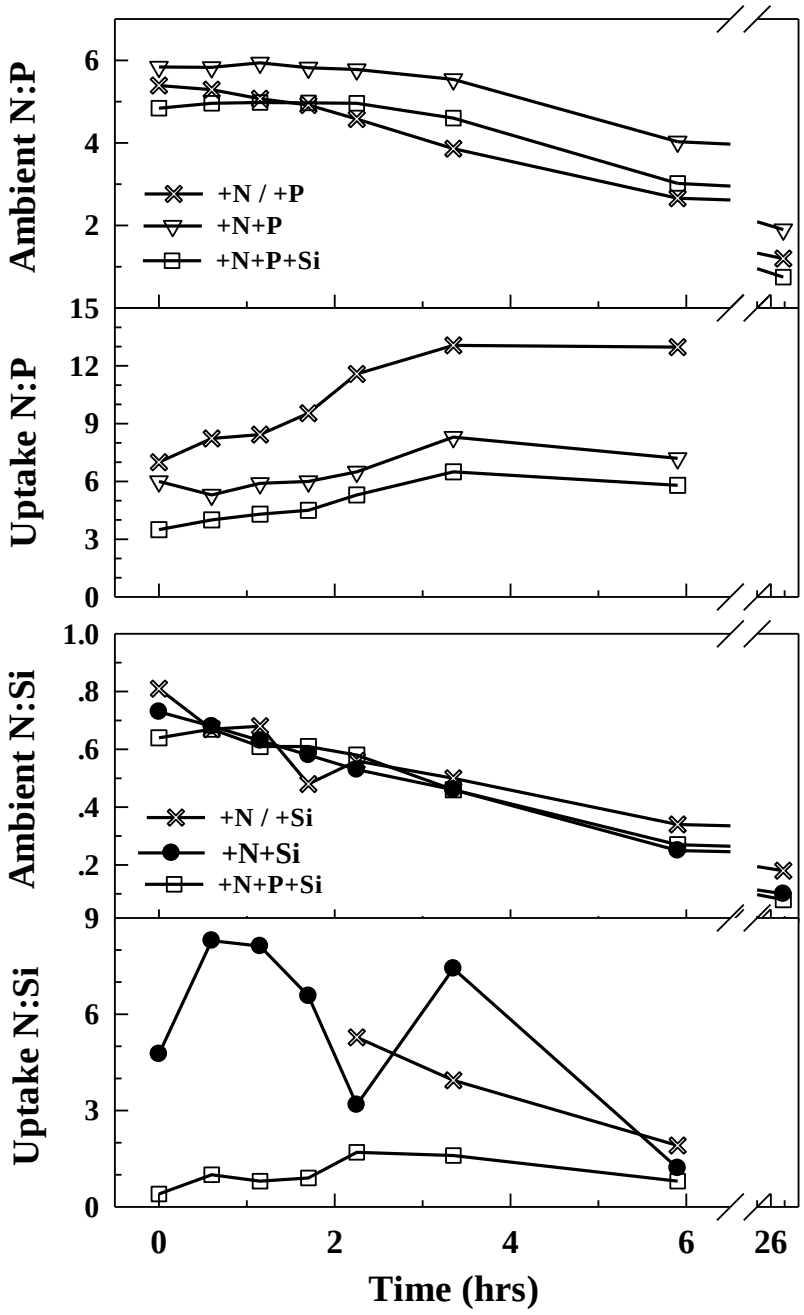
Ambient N:P
Uptake N:P
Ambient N:Si
Uptake N:Si
+N / +P
+N+P
+N+P+Si
+N / +Si
+N+Si
+N+P+Si
Time (hrs)

Fig. 10

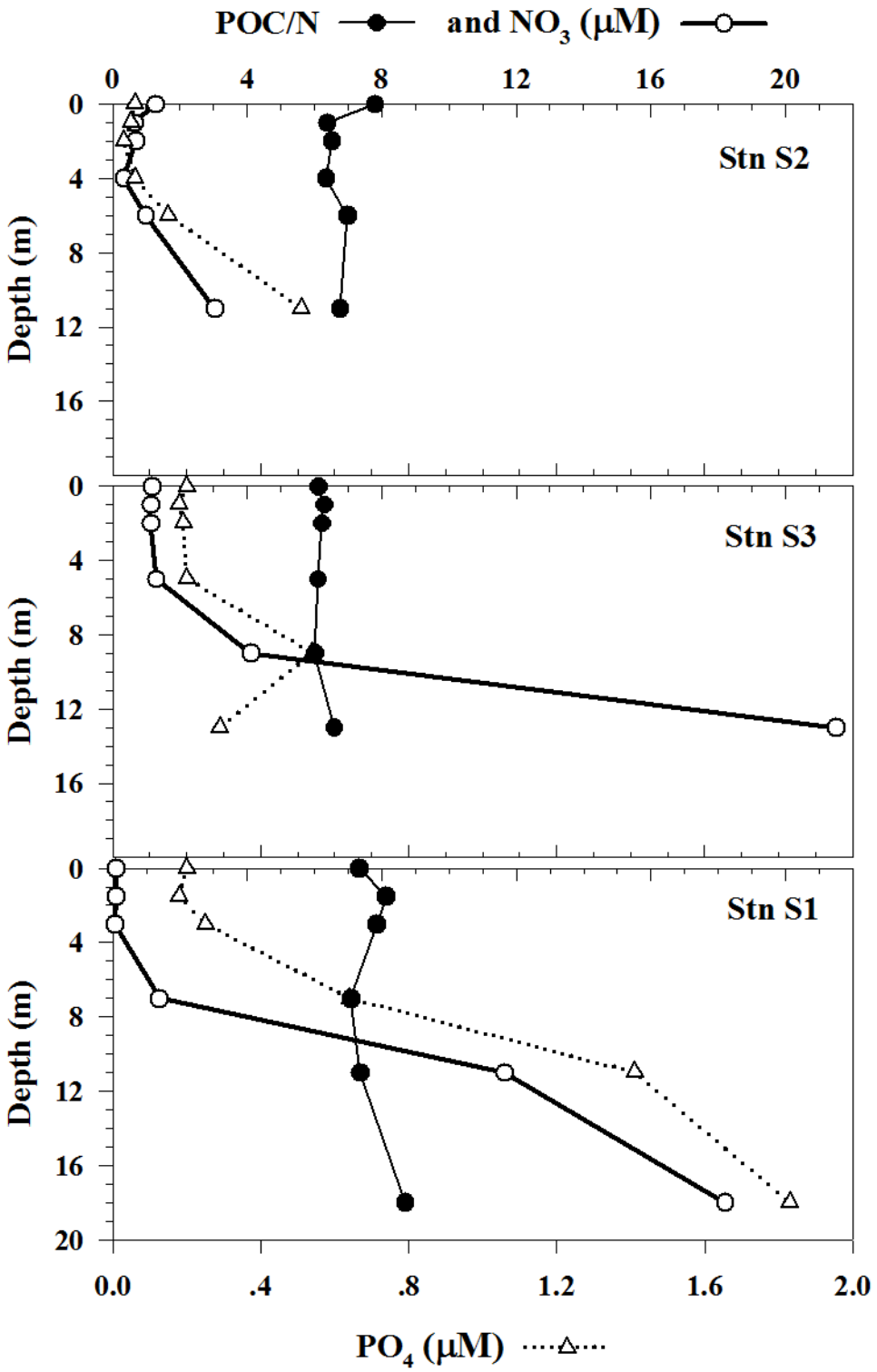
POC/N
and NO3 (µM)
0
4
8
12
16
20
Stn S2
Stn S3
Stn S1
Depth (m)
0
4
8
12
16
20
0.0
.4
.8
1.2
1.6
2.0
PO4 (µM)